

## Modification of polyvinylidene fluoride membrane by blending with cationic polyionic liquid

Linbin Zhang<sup>a</sup>, Shusu Shen<sup>a,b,\*</sup>, Yiyuan Zhang<sup>a</sup>, Xiaoji Zhou<sup>a,b</sup>, Renbi Bai<sup>a,b,\*</sup>

<sup>a</sup>Center for Separation and Purification Materials & Technologies, Suzhou University of Science and Technology, Suzhou, China, Tel. +86 51268092987; emails: shusushe@mail.usts.edu.cn (S. Shen), brb998@outlook.com (R. Bai), 2778418673@qq.com (L. Zhang), 1585305056@qq.com (Y. Zhang), 359300091@qq.com (X. Zhou)

<sup>b</sup>Jiangsu Collaborative Innovation Center for Technology and Material of Water Treatment, Suzhou University of Science and Technology, Suzhou, China

Received 3 September 2019; Accepted 5 February 2020

### ABSTRACT

Fouling problem is now the bottleneck in the wide application of membrane technology in the water and waste-water treatments, and membrane antifouling modifications have been well developed recently. In this paper, positively charged porous membranes were prepared by blending a cationic polyionic liquid (PIL) and polyvinylpyrrolidone with polyvinylidene fluoride (PVDF). Increased surface hydrophilicity (water contact angle of 54.07°) and enlarged pure water flux (764.8 L/m<sup>2</sup> h bar) were detected. The obtained blend membranes with cationic PIL showed obvious positive charge whilst the pristine PVDF was negatively charged. Filtration tests of bovine serum albumin (BSA) solution at pH 3.6 indicated that the blend membranes showed an enhanced antifouling property (75.3% of flux recovery rate) due to the positively charged surface.

*Keywords:* Membrane modification; Polyionic liquid; Hydrophilicity; Positively charged membrane; Anti-fouling property

### 1. Introduction

Membrane technology has gradually demonstrated its advantages in water and waste-water treatments [1,2]. Polyvinylidene fluoride (PVDF) is regarded as the oldest and widely used membrane material due to its good film-forming properties, simple preparation process, low price, etc., [3]. However, the fouling problem restricts the fast development of PVDF membrane in water treatment. Studies on PVDF membrane modification have been developed well, most of them are hydrophilic modification [4,5] because the PVDF membrane is hydrophobic (~80° of water contact angle). Hydrophilic membranes help the formation of a thin hydration layer between the membrane surface and contaminants in water, inhibiting the direct contact of contaminants onto the membrane.

Besides the hydrophilic modifications, surface charge modification [6] also can be utilized. Because most of the contaminants in water are charged, for example, the proteins in wastewater can be positive charge or negative charge at different pH. By carrying out the membrane charge modification, the pore size screening effect and the charge repulsion effect may work synergistically during the separation of pollutants from water, especially to the charged pollutants. Lin et al. [7] developed a negatively charged function on the PVDF membrane by irradiation graft modification. Therefore, it is repelled from the negatively charged oil and suspended matter in the oily sewage, so that the crude oil does not adhere to the membrane, thereby prolonging the service life of the membrane. Zhao et al. [8] immersed the oxidized PVDF membrane into an aqueous acrylic acid solution to carry out surface graft polymerization to provide a

\* Corresponding authors.

polyacrylic acid surface-modified PVDF membrane. It is then placed into a polyanionic electrolyte solution, a polycationic electrolyte solution or a zwitterionic betaine-based polymer solution for adsorption to prepare a porous PVDF membrane having a different charged surface.

Compared with the surface grafting or surface coating modifications, the blending method demonstrates the advantages that the prepared membrane has good uniformity and the process is easy to handle and favorable for industrial production. In blending modified materials, polyionic liquids (PILs) combine the dual properties of ionic liquids (ILs) and polymers [9,10]. They have been widely applied in fabricating functional materials, such as carbon dioxide adsorbent materials [11], polyelectrolytes [12]. Du et al. [13] reported a charged block PIL brush copolymer, poly(methyl methacrylate-*b*-1-[(2-methacryloyloxy)ethyl]-3-butylimidazolium bromine) P(MMA-*b*-MEBIm-Br), and blended it with PVDF to prepare an ion-sensitive PVDF membranes. However, the pure water flux in the report was low, and the maximum pure water flux was 343 L/m<sup>2</sup>h.

Polyvinylpyrrolidone (PVP) usually acts as a mature porogen and can be added in the preparation of porous membranes. The addition of PVP into the casting solution system results in a larger and looser pore structure during membrane phase transformation, which is quite useful for the improvement of membrane water flux [14,15] and enhances the anti-pollution performance of the membranes [16]. The addition of PVP was also reported to help the anti-aging and anti-erosion performance during the actual operation of the membrane module [17].

In this study, a cationic PIL obtained in our lab, poly(polyethylene glycol methacrylate-*co*-1-butyl-3-vinylimidazolium bromide) [P(PEGMA-*co*-BVIIm-Br)] (Fig. 1), and porogen PVP were both added into the blending of PVDF membranes to prepare the positively charged membranes. The modification effects including the hydrophilicity and the antifouling properties were carefully explored.

## 2. Experimental

### 2.1. Materials and reagents

PVDF (FR 904, >99.5%, M<sub>w</sub> = 400,000), 3F New Materials Co. Ltd., Neimenggu, China; PVP (>99.0%), Tianjin Zhiyuan

Chemical Reagent. The above chemicals were dried before use. Polyethylene glycol methacrylate (PEGMA), Sigma-Aldrich, Shanghai, China; 1-Vinylimidazole (C<sub>5</sub>H<sub>6</sub>N<sub>2</sub>, 99%), 1-bromobutane (C<sub>4</sub>H<sub>9</sub>Br, >99%), N,N-dimethylformamide (DMF, AR), and azobisisobutyronitrile (AIBN, 98%), Macklin Biochemical Technology (Shanghai, China); bovine serum albumin (BSA, M<sub>n</sub> = 67 kDa), Aladdin Biochemistry Technology (Shanghai, China). Petroleum ether and other reagents are analytical reagent grades from Jiangsu Qiangsheng. All reagents were used as received without further purification, and the desired solution was prepared in all experiments using Millipore's Milli-Q system purified deionized water (18.2 MΩ).

### 2.2. Preparation of blend PVDF membrane

The PIL P(PEGMA-*co*-BVIIm-Br) (Fig. 1) was synthesized via a reversible addition-fragmentation chain transfer (RAFT) polymerization between PEGMA and 3-butyl-1-vinyl-1H-imidazol-3-ium bromide (BVIIm-Br). The BVIIm-Br was synthesized from the addition reaction [18] between 1-vinylimidazole (C<sub>5</sub>H<sub>6</sub>N<sub>2</sub>) and 1-bromobutane (C<sub>4</sub>H<sub>9</sub>Br). PEGMA (8 mmol), BVIIm-Br (4 mmol), and AIBN (0.06 mmol) were mixed in 10 mL of DMF under nitrogen protection. The mixture was stirred at 65°C for 24 h. After stopped the reaction in an ice-water bath, the mixture was allowed to settle in petroleum ether and gave a pale yellow viscous liquid which was further purified by dissolving it in dichloromethane and resettled in petroleum ether. The crude was concentrated in vacuum to give P(PEGMA-*co*-BVIIm-Br) as a pale yellow viscous liquid.

Flat membrane was prepared by an immersion precipitation phase inversion method (L-S method). The dried PVDF was dissolved in DMF in a certain weight ratio (Table 1) with the obtained PIL P(PEGMA-*co*-BVIIm-Br) and PVP for 24 h. After that, the obtained casting solution was cooled to room temperature and left to defoam. The defoamed casting solution was spread onto a clean, dry glass with a knife thickness of 300 μm, and was placed into DI water at 30°C. Then, the obtained membrane was moved to a fresh DI water (room temperature) for 48 h, and finally naturally dried. The membrane samples were stored at desiccator for further tests.

### 2.3. Characterization of the membranes

#### 2.3.1. Surface chemical composition analysis

An attenuated total reflectance-Fourier-transform infrared spectroscopy (ATR-FTIR) spectrometer (Thermo Fisher 6700, USA) was used to investigate the functional groups on the membrane surface.

#### 2.3.2. Membrane morphology and pore size distribution

The morphologies of the prepared membranes were observed with a scanning electron microscope (SEM, Phenom Pro). The surfaces and cross-sections of the prepared membrane samples were scanned for the SEM images with an excitation voltage of 5 kV.

The average pore size was measured by a specific surface area and pore size analyzer (V-Sorb 2800TP), and was determined byBJH model calculation method.

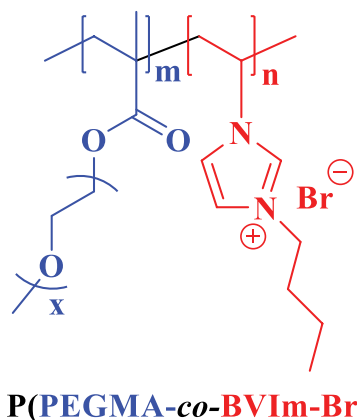


Fig. 1. Chemical structure of P(PEGMA-*co*-BVIIm-Br).

Table 1  
Composition of the casting solutions of the membranes

Membrane	PVDF (wt.%)	Additive (wt.%)	Ratio of PVDF/Additive	PVP (wt.%)	DMF (wt.%)
Pristine PVDF	15	None	None	None	85.0
M1	15	None	None	2	83.0
M2	15	PEGMA (8)	15/8	2	75.0
M3	15	P(PEGMA-co-BVIm-Br) (6)	15/6	2	77.0
M4	15	P(PEGMA-co-BVIm-Br) (8)	15/8	2	75.0

### 2.3.3. Water contact angle and mechanical properties

The water contact angles (WCAs) of the membranes were tested using a contact angle goniometer (Ramé-Hart 500) through the static sessile drop method. Several measurements at different locations of each sample were made, at least five data for each sample were collected and the average value of the measurements with an error less than 3° was used as the representative WCA of the tested membranes. Tensile strengths and tensile strains at the breaks of the membrane samples were measured using an electronic tensile testing machine (Instron 5944, USA) operated at room temperature with a strain rate of 1 cm/min. For each condition used, the average value of at least three tests was reported.

### 2.3.4. Surface zeta potential measurement

The surface charge properties of the membrane were measured by a flow potential method. Flow potential measurements were made using a membrane/solid sample flow field potential analyzer (Surpass, Anton-Paar, USA). The zeta potential of the membrane was measured using a 1.0 mM KCl solution.

### 2.4. Membrane permeability and anti-protein tests

Membrane permeability was evaluated by using a dead-end filtration system. All membrane samples were pressurized with DI water at trans-membrane pressure of 0.15 MPa for 30 min until membrane performance was stable. The constant flux was recorded as  $J_w$  at 0.1 MPa. Each sample was measured three times with the average values as the membrane water flux. The pure water flux ( $J_w$ ) was estimated by the following equation:  $J_w = V/(A \times \Delta t)$ , where the parameters  $V$ ,  $A$ , and  $\Delta t$  were defined as the DI water or permeate volume (L), membrane area (m<sup>2</sup>), and permeation time (h), respectively.

Anti-protein tests were performed by filtration of a serial of BSA solutions at different pH conditions. A 1.0 g/L BSA solution was prepared by dissolving 1 g BSA in 1 L of 100 mM buffer solution. Where, the buffer (pH 3.6) was prepared by dissolving 5.6 g acetic acid and 0.5 g anhydrous sodium acetate in 1 L DI water.

After obtaining the pure water flux ( $J_w$ ) for the selected membrane, the prepared BSA solution was pressurized at 0.10 MPa to filtrate through the membrane, and the flux after 120 min was recorded as  $J_p$ . After rinsing the membrane with DI water, it was then put back into the system

and the stable pure water flux was measured again and recorded as  $J_r$ .

The relative flux decay (RFD) was calculated by  $RFD = [(J_w - J_p)/J_w] \times 100\%$ , and the flux recovery ratio (FRR), indicating the extent of the possible reversible fouling, was calculated by  $FRR = (J_r/J_w) \times 100\%$ . The BSA retention or rejection rate ( $R$ ) was calculated by the equation  $R_{BSA} = (1 - C_1/C_0) \times 100\%$ . Where  $C_0$  and  $C_1$  are the concentrations of proteins in the solution before and after filtration, respectively, measured by a UV-vis spectrometer, at a wavelength of 280 nm.

## 3. Results and discussion

### 3.1. Chemical composition of the membrane surface

The surface chemical composition of different membranes (Table 1) were analyzed by ATR-FTIR. As shown in Fig. 2, 3,020 and 2,980 cm<sup>-1</sup> were C–H stretching vibrations, and 1,402 cm<sup>-1</sup> attributed to the deformation rocking vibration of CH<sub>2</sub> [19]. The peak of 1,170 cm<sup>-1</sup> should be the CF<sub>2</sub> stretching vibration, and sharp absorption at 1,070 cm<sup>-1</sup> was assigned to vibration absorption peak of the crystal phase [20]. There were obvious observations of carbonyl group (C=O) at 1,724 cm<sup>-1</sup> [21] for blend membranes M3 and M4, this attributed to the carbonyl group in the additive polymer P(PEGMA-co-BVIm-Br), and the adsorption peaks were enhanced with the increasing additive. The peak observation at 1,662 cm<sup>-1</sup> attributed to the carbonyl group of amide in

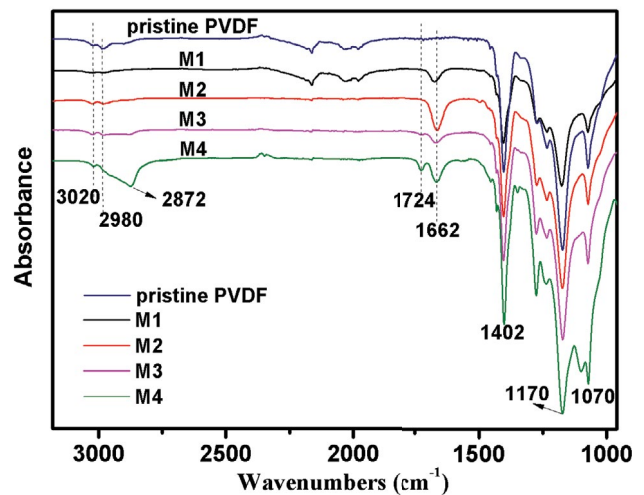


Fig. 2. FTIR spectra of the membranes.

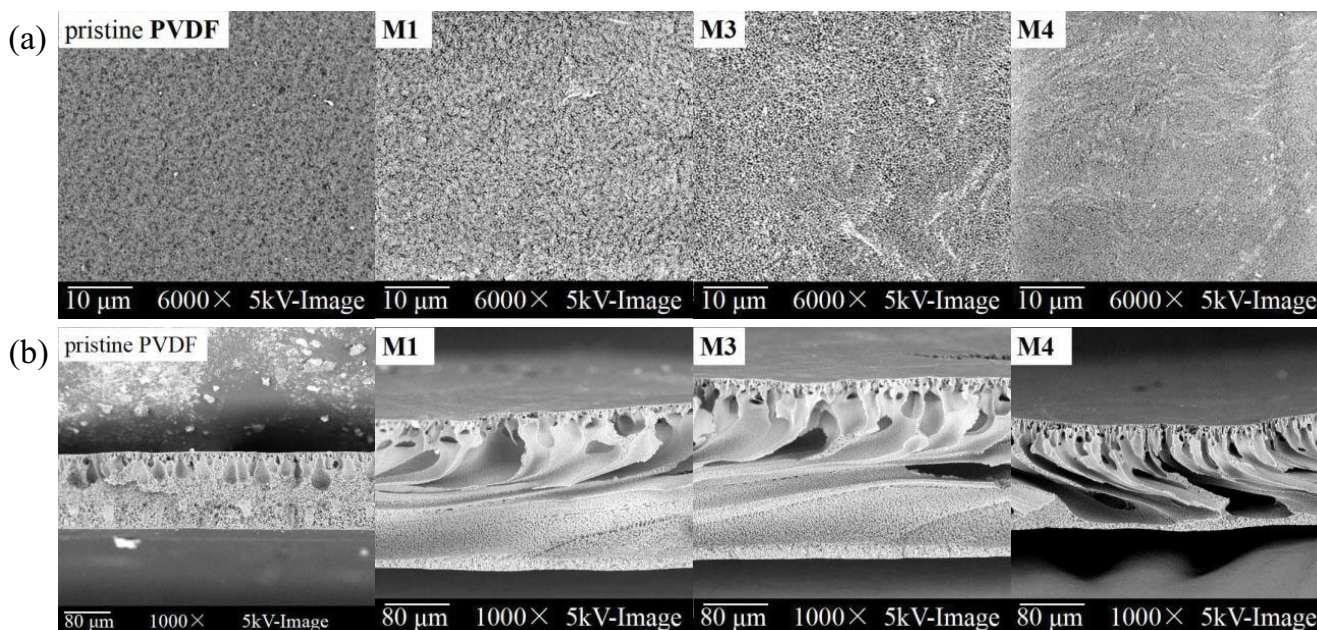


Fig. 3. Surface (a) and cross-sectional (b) SEM images of the membranes.

PVP. Although the carbonyl group exists in PEGMA, there was no obvious adsorption peak of carbonyl group in the surface IR spectrum of the blend membrane M2 (6 wt.% of PEGMA). This may be caused by the good solubility of PEGMA in water, and most of the added PEGMA moved to the coagulation bath (DI water) during the membrane formation. Comparably, most of the synthesized P(PEGMA-co-BVIm-Br) retained well on the membrane surface.

### 3.2. Membrane morphology and pore size distribution

The SEM images of the blend membranes are shown in Fig. 3, and the pore size data are listed in Table 2. It can be found in Fig. 3a that, the pores on the surface of the pristine PVDF membrane were unevenly distributed and the pore sizes were different. The pristine PVDF (M1) containing PVP had a significantly increased upper surface pore diameter (Table 2, 84.02 nm). The surface pores of the blend membrane M3 and M4 were more and more uniform than M1, the pore sizes were increased to 92.36 nm for M4 with the more additive.

As shown in Fig. 3b, the skin layer for pristine PVDF membrane was dense, and it was supported by a thick sponge layer. By mixing PVP into the mixture, the cross-section of the membranes became thicker and looser, more finger-like pores were observed. With the addition of PIL, more macro-voids were formed. The appearance of macro-porous structures indicated that the additive in the blend membrane accelerated the solvent-nonsolvent diffusion rate, thus accelerating the transient liquid-liquid phase separation of PVDF and solution [22].

### 3.3. Water contact angle and mechanical strength

As summarized in Table 3, the water contact angle (WCA) for pristine PVDF membrane was 77.75°. The PVP

Table 2  
Average pore diameter of the membranes

Membranes	Average pore diameter (nm)
Pristine PVDF	17.61
M1	84.02
M3	91.87
M4	92.36

addition into PVDF decreased the WCA of M1 to 63.88°, because the porogen helped the formation of membrane porous structure, and it has been described in the previous part that the average pore sizes of M1 was much larger than pristine PVDF membrane, and this is quite good for the water affinity. The WCA of Membrane M2 (61.89°) who was prepared from blending 6 wt.% PEGMA was similar as M1, this can be explained from the FTIR analysis that there was seldom PEGMA were observed on the membrane surface. However, the PIL, P(PEGMA-co-BVIm-Br) greatly affected the membrane hydrophilicity. The WCAs of the blend membranes gradually decreased, and the WCA of M4 became 54.07°. It has been proved that PIL retained on the membrane surface by the FTIR analysis. Therefore, the synthesized P(PEGMA-co-BVIm-Br) demonstrates a good hydrophilic property and acts as an efficient hydrophilic modifier. However, with the addition of PVP or PIL, the mechanical properties of the membranes were damaged. The tensile stress was decreased from 1.43 to 0.55 MPa, and the elongation was dropped from 20.4% to 10.5%, this may be explained by the compatibility between the blend materials. This can be predicted from the SEM images that more macro-voids were found for the blend membranes M3 and M4, which is unfavorable to the mechanical properties.

Table 3  
Basic properties of the membranes

Membranes	Water contact angle (°)	Mechanical strength		Pure water flux (L/m <sup>2</sup> h-bar)
		Tensile stress (MPa)	Elongation (%)	
Pristine PVDF	77.75 ± 2.63	1.43	20.4	17.2 ± 0.9
M1	63.88 ± 2.35	0.93	19.6	478.1 ± 5.6
M2	61.89 ± 1.64	0.55	14.5	Untested
M3	54.80 ± 1.84	0.66	14.1	699.2 ± 6.5
M4	54.07 ± 0.43	0.52	10.5	764.8 ± 9.5

### 3.4. Water flux analysis

The water flux of the pure PVDF membrane increased greatly from 17.2 to 478.1 L/m<sup>2</sup> h bar due to the addition of the porogen PVP. With the increase of the amount of copolymer added, the water flux of the blend membrane M3 and M4 also increased, and the water flux of membrane M4 reached a maximum of 764.8 L/m<sup>2</sup> h bar. It is indicated that as the amount of copolymer added increases, the surface of the blend membrane is provided with a hydrophilic group. At the same time, the porogen PVP changed the internal structure of the membrane, resulting in an increase in the pore size in the membrane (Table 2) which benefits the improved water flux.

### 3.5. Zeta potentials

As shown in Fig. 4, the surface of the pristine PVDF membrane was negatively charged at a pH of 2–12, and the membrane surfaces of M1 and M2 were also negatively charged. The surfaces of the blend membranes M3 and M4 were positively charged, this is because the imidazole group in the synthesized P(PEGMA-co-BVIm-Br) was positive and made the cationic P(PEGMA-co-BVIm-Br) positively charged, finally enriched at the membrane surface. However, as the content of P(PEGMA-co-BVIm-Br) in the blend membrane increased, the surface charge of the membrane did not increase obviously. It is proposed that the blend membrane was not only surface-charged because the large pore size of the blend membrane was observed (Table 2), but also internal charged, the excessive addition of the cationic PIL did not greatly enhance the surface charge of the membrane.

### 3.6. Anti-protein performance

The prepared membranes were tested for filtration by using a typical protein, BSA. BSA has an isoelectric point (pI) at 4.7, a positive charged BSA could be obtained at solution pH < 4.7. The antifouling ability of the modified membranes M1, M3, and M4 were evaluated by the BSA solution at pH 3.6. The flux change of the membranes are illustrated in Fig. 5, and the corresponding FRD, FRR, and R of the membranes during filtration of BSA Filtration are summarized in Table 4.

As shown in Fig. 5, the pure water flux ( $J_w$ ) of the membrane M1 was 478.1 L/m<sup>2</sup> h bar, it is much greater than that of pristine PVDF (17.2 L/m<sup>2</sup> h bar). This huge improvement

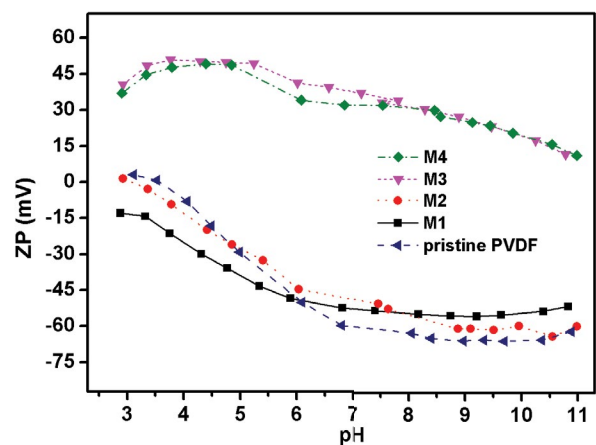


Fig. 4. Zeta potential diagram of the membranes at different pH values ( $C_{KCl} = 1$  mM).

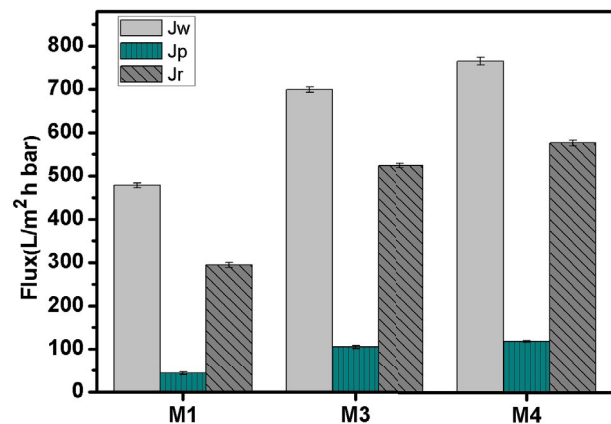


Fig. 5. Flux change of the membranes during filtration of BSA (room temperature, 0.1 MPa, pH = 3.6).

was caused by the addition of PVP that a more porous membrane structure was formed. With addition of PIL, the blend membrane gave a water flux at 699.2 L/m<sup>2</sup> h bar, and membrane M4 who has the higher content of PIL gave the highest water flux at 764.8 L/m<sup>2</sup> h bar. This result is accorded to the previous SEM and pore size analysis that more macro-voids

Table 4  
FRD, FRR, and *R* of the membranes

Membrane	<i>R</i> (%)	FRD (%)	FRR (%)
M1	14.6 ± 0.2	38.4 ± 5.4	61.6 ± 9.5
M3	19.8 ± 0.2	25.1 ± 2.9	74.9 ± 7.1
M4	22.0 ± 0.6	24.7 ± 3.2	75.3 ± 6.8

were detected for M3 and M4, and the pore size of M3 and M4 were bigger than M1. That is, by adding PVP and P(PEGMA-co-BVIm-Br), the water flux of the modified PVDF membranes have been dramatically improved, which is necessary for the practical water or waste-water treatment.

It has been mentioned that M3 and M4 had larger pore size than M1, where, the pore size screening effect for M3 and M4 were smaller than M1, but higher rejections were observed for membranes M3 (19.8%) and M4 (22.0%) than M1 (14.6%), as shown in Table 4. Therefore, during the filtration of BSA solution for modified membranes M3 and M4, instead of the pore size screening effect, the electrostatic repulsion between the positive BSA and the positive membrane surface should be the major separation mechanism. M4 showed the best rejection because of the higher content of P(PEGMA-co-BVIm-Br) in the blend PVDF membrane and the relatively more positive charged membrane surface.

As shown in Fig. 5, although the initial pure water flux ( $J_w$ ) of the modified membranes were very high, after filtration of BSA solutions, the flux ( $J_p$ ) dropped to 42.6, 105.1, and 117.6 L/m<sup>2</sup> h bar for M1, M3, and M4, respectively. And, 38.4%, 25.1%, and 24.7% of FRD were calculated for the membranes, the modified membrane M4 gave the lowest flux relative decay. After a simple water flushing, the water fluxes ( $J_p$ ) for each membrane were recovered to 294.6, 523.6, and 575.8 L/m<sup>2</sup> h bar, respectively. And, the FRR were 61.6%, 74.9%, and 75.3%, in which, membrane M4 still showed the highest flux recovery. Therefore, M4 who is fabricated from the higher ratio of P(PEGMA-co-BVIm-Br) in the blending with PVDF demonstrated the best antifouling ability. Both the greater hydrophilicity and higher positive charge on the membrane surface resulted in the good antifouling property. The greater hydrophilicity helps the formation of hydration layer on the membrane surface that can resist the contact of the contaminants, and the higher positive charge further strengthens the repulsion between the positive membrane surface and the positive pollutants.

#### 4. Conclusions

In this study, positively charged porous PVDF membranes were fabricated from the blending of the cationic P(PEGMA-co-BVIm-Br) and PVP with PVDF. The addition of PVP and PIL into the PVDF membrane greatly improved the membrane hydrophilicity, the water contact angle was reduced from 77.75° of pristine PVDF membrane to 54.07°. A huge improvement of pure water flux was found for the modification that the water flux was increased from 17.2 to 764.8 L/m<sup>2</sup> h bar, which is quite favorable for practical application. By adding the cationic PIL into the PVDF, the blend

membrane showed a positive surface while the pristine PVDF membrane was negatively charged. During the filtration of the positive BSA molecules at solution pH 3.6, with the assistance of the electronic repulsion between the positive membrane surface and positive pollutant, the rejection rate, FRD, and FRR were enhanced. The positively charged PVDF membrane with a higher content of cationic PIL showed improved antifouling performance.

#### Acknowledgments

Thanks to the financial support from the National Natural Science Foundation of China (No. 51608342) and Pre-research Fund of Jiangsu Collaborative Innovation Center of Technology and Material of Water Treatment (XTCXSZ2019-4).

#### References

- [1] J. Guo, M.U. Farid, E.J. Lee, D.Y.S. Yan, S. Jeong, A.K. An, Fouling behavior of negatively charged PVDF membrane in membrane distillation for removal of antibiotics from wastewater, *J. Membr. Sci.*, 551 (2018) 12–19.
- [2] S. Zhang, R. Wang, S. Zhang, G. Li, Y. Zhang, Treatment of wastewater containing oil using phosphorylated silica nanotubes (PSNTs)/polyvinylidene fluoride (PVDF) composite membrane, *Desalination*, 332 (2014) 109–116.
- [3] G.D. Kang, Y.M. Cao, Application and modification of poly(vinylidene fluoride) (PVDF) membranes—a review, *J. Membr. Sci.*, 463 (2014) 145–165.
- [4] X. Zhu, H.E. Loo, R. Bai, A novel membrane showing both hydrophilic and oleophobic surface properties and its non-fouling performances for potential water treatment applications, *J. Membr. Sci.*, 436 (2013) 47–56.
- [5] F. Chen, X. Shi, X. Chen, W. Chen, Preparation and characterization of amphiphilic copolymer PVDF-g-PMABS and its application in improving hydrophilicity and protein fouling resistance of PVDF membrane, *Appl. Surf. Sci.*, 427 (2018) 787–797.
- [6] C. Liu, W. Bi, D. Chen, S. Zhang, H. Mao, Positively charged nanofiltration membrane fabricated by poly(acid-base) complexing effect induced phase inversion method for heavy metal removal, *Chin. J. Chem. Eng.*, 25 (2017) 1685–1694.
- [7] A. Lin, S. Shao, H. Li, D. Yang, Y. Kong, Preparation and characterization of a new negatively charged polytetrafluoroethylene membrane for treating oilfield wastewater, *J. Membr. Sci.*, 371 (2011) 286–292.
- [8] X. Zhao, H. Xuan, A. Qin, D. Liu, C. He, Improved antifouling property of PVDF ultrafiltration membrane with plasma treated PVDF powder, *RSC Adv.*, 79 (2015) 64526–64533.
- [9] J. Yuan, M. Antonietti, Poly(ionic liquid)s: polymers expanding classical property profiles, *Polymer*, 52 (2011) 1469–1482.
- [10] D. Cordella, A. Kermagoret, A. Debuigne, R. Riva, I. German, M. Isik, C. Jérôme, D. Mecerreyes, D. Taton, C. Detrembleur, Direct route to well-defined poly(ionic liquid)s by controlled radical polymerization in water, *ACS Macro Lett.*, 3 (2014) 1276–1280.
- [11] N. Sahiner, S. Demirci, Poly ionic liquid cryogel of polyethyleneimine: synthesis, characterization, and testing in absorption studies, *J. Appl. Polym. Sci.*, 133 (2016) 43478.
- [12] S. Imaizumi, Y. Kato, H. Kokubo, M. Watanabe, Driving mechanisms of ionic polymer actuators having electric double layer capacitor structures, *J. Phys. Chem. B*, 116 (2012) 5080–5089.
- [13] C. Du, X. Ma, J. Li, C. Wu, Improving the charged and antifouling properties of PVDF ultrafiltration membranes by blending with polymerized ionic liquid copolymer P(MMA-b-MEBIm-Br), *J. Appl. Polym. Sci.*, 134 (2017) 44751.
- [14] H. Matsuyama, T. Maki, M. Teramoto, K. Kobayashi, Effect of PVP additive on porous polysulfone membrane formation by

- immersion precipitation method, *Sep. Sci. Technol.*, 38 (2003) 3449–3458.
- [15] P. Moradihamedani, A.H. Bin Abdullah, Phosphate removal from water by polysulfone ultrafiltration membrane using PVP as a hydrophilic modifier, *Desal. Water Treat.*, 57 (2016) 25542–25550.
- [16] M.O. Mavukkandy, M.R. Bilad, A. Giwa, S.W. Hasan, H.A. Arafat, Leaching of PVP from PVDF/PVP blend membranes: impacts on membrane structure and fouling in membrane bioreactors, *J. Mater. Sci.*, 51 (2016) 4328–4341.
- [17] Y. Kourde-Hanafi, P. Loulergue, A. Szymczyk, B.V.D. Bruggen, M. Nachtnebel, M. Rabiller-Baudry, J.L. Audic, P. Pölt, K. Baddari, Influence of PVP content on degradation of PES/PVP membranes: insights from characterization of membranes with controlled composition, *J. Membr. Sci.*, 533 (2017) 261–269.
- [18] M. Andersson, Ö. Hansson, L. Öhrström, A. Idström, M. Nydén, Vinylimidazole copolymers: coordination chemistry, solubility, and cross-linking as function of  $\text{Cu}^{2+}$  and  $\text{Zn}^{2+}$  complexation, *Colloid Polym. Sci.*, 289 (2011) 1361–1372.
- [19] S. Al-Gharabli, W. Kujawski, Z. Abu El-Rub, E.M. Hamad, J. Kujawa, Enhancing membrane performance in removal of hazardous VOCs from water by modified fluorinated PVDF porous material, *J. Membr. Sci.*, 556 (2018) 214–226.
- [20] Z. Peng, L.X. Kong, S.D. Li, Non-isothermal crystallisation kinetics of self-assembled polyvinylalcohol/silica nanocomposite, *Polymer*, 46 (2005) 1949–1955.
- [21] T. Li, F. Liu, H. Lin, Z. Xiong, H. Wang, Y. Zhong, L. Xiang, A. Wu, Fabrication of anti-fouling, anti-bacterial and non-clotting PVDF membranes through one step “outside-in” interface segregation strategy, *J. Colloid Interface Sci.*, 517 (2018) 93–103.
- [22] N.A. Hashim, F. Liu, K. Li, A simplified method for preparation of hydrophilic PVDF membranes from an amphiphilic graft copolymer, *J. Membr. Sci.*, 345 (2009) 134–141.